A Model for the Devolatilization of EPDM Rubber in a Series of Steam Stripping Vessels

Angelica J. B. Francoeur, Hadiseh Karimi, and Kim B. McAuley
Dept. of Chemical Engineering, Queen's University, Kingston, Canada K7L3N6

Luigi D'Agnillo
LANXESS Elastomers BV, Geleen, The Netherlands

DOI 10.1002/aic.14448
Published online April 1, 2014 in Wiley Online Library (wileyonlinelibrary.com)

A mathematical model was developed for the multitank stripping section of industrial ethylene propylene diene monomer (EPDM) rubber processes. Experiments were conducted to determine Henry's law coefficients and diffusivities for hexane solvent and 5-ethylidene-2-norbornene (ENB) comonomer in EPDM particles. Equivalent radii for diffusion within the particles were also determined. A model was developed to predict solvent and comonomer concentrations in a single particle as it moves through a series of tanks with different operating conditions. A second, more-complicated model was then developed to account for a continuous flow stirred tank residence time distribution for the particles in the tanks. Data from three industrial plants were used to estimate parameters and assess the models' predictive ability. Typical prediction errors are 0.90 wt % for residual hexane and 0.14 wt % for residual ENB. © 2014 American Institute of Chemical Engineers *AIChE J*, 60: 2596–2606, 2014

Keywords: mathematical modeling, steam stripping, rubber, ethylene propylene diene monomer solvent removal

Introduction

Polymer latexes and slurries commonly contain residual of unreacted monomers and solvent. As a result,[1] removal of volatile organic compounds (VOCs) is important due to health, safety, and environmental concerns.[1,2] Several physical and chemical processes can be used to separate solvent from polymers.[3–6] In devolatilization processes, the latex is stripped using steam or gas.[5] Despite the industrial importance of the devolatilization, mathematical models able to predict removal of VOCs from polymer latexes and slurries are rare in the literature.[6]

In this article, a mathematical model is developed to predict removal of VOCs from ethylene propylene diene monomer (EPDM) rubber particles in the stripping section of an industrial EPDM production process. EPDM is a high-density rubber that has a wide range of applications in seals for doors and windows, hoses, tubing, electrical insulation, and roofing membranes.[7–10] The "M" in EPDM sometimes refers to the methyl backbone of the polymer as described in the ASTM standard.[11,12] The structure for a generic EPDM rubber is given in Figure 1. Several different diene monomers are used commercially including 5-ethylidene-2-norbornene (ENB) and dicyclopentadiene (DCPD) (see Figure 2).[5] Note that ENB comonomer was used to produce the particular EPDM shown in Figure 3.

Industrially, EPDM is commonly polymerized in a hexane solution.[13] Multitank steam stripping is used for the removal of residual comonomers and hexane from EPDM rubber particles. In this process, the rubber solution is briefly contacted with water to form particles (crumb) and immediately directed into a vessel of boiling water, where most of the hexane evaporates (see Figure 4). The crumb slurry exiting this first stripping vessel is then fed to a succession of vessels to remove the remaining volatiles. Each stripping tank in the series is agitated and fed with steam to control the temperature.[11,14] High recovery of solvent and residual comonomer from the rubber particles is essential.[15] Optimization of steam-stripping system requires an accurate model that can predict residual solvent and comonomer concentrations in rubber crumb leaving the successive tanks.

Several mathematical models have been developed to describe solvent or residual comonomer removal from rubber particles under different operating conditions.[14–19] Matthews et al.[19] developed a model to describe diffusion of hexane solvent from EPDM particles. They proposed that mass transfer from the particles could best be described by Fickian diffusion from smaller solid particles within the larger porous rubber particle, and that the estimated "effective radius of diffusion" of ~1 mm corresponds approximately to the diameter of particles visible within the porous crumb. Matthew's model also accounts for the influence of solvent concentration on the diffusivity coefficient for EPDM. In another study, Matthews et al.[15] extended their model to a continuous flow stirred tank (CFST) stripping system. In Matthew's extended model, a residence time distribution for a CFST was incorporated to account for the different times that individual crumb particles spend in a single stripping vessel. Later, Cozewith[18] extended the models of Matthews et al.[15,19] to predict residual concentrations in crumb

Correspondence concerning this article should be addressed to K. B. McAuley at kim.mcauley@chee.queensu.ca.

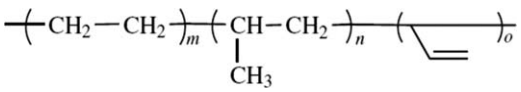

Figure 1. EPDM polymer structure with an aliphatic comonomer.[11]

Note that the various monomers are arranged randomly in the EPDM rubber.

particles emerging from a series of two or more stripping vessels. Cozewith assumed that the residence times are the same for all of the tanks in series. Additionally, Cozewith's tanks-in-series model requires the user to assume either that stripping conditions (i.e., temperature and solvent partial pressures) are the same in all tanks, or that the inlet concentrations of solvent and comonomer are much higher in the initial crumb than would be encountered in the tanks if equilibrium was obtained between particles and the headspace. These assumptions are not valid during typical industrial operation. Quadri[14] extended Cozewith's model to include ordinary differential equations that describes a thin well-mixed boundary layer in the liquid phase. These equations account for mass-transfer resistance in the liquid. As a result, Quadri's model requires additional mass-transfer parameters. Note that the use of Cozewith's model requires information about the equivalent radius for diffusion, the equilibrium partitioning of solvent and comonomers between the gas phase and the rubber particles, and diffusivities of solvent and comonomer within the rubber. The values used by Matthews et al., Cozewith and Quadri are not accurate for the range of EPDM grades and industrial stripping conditions that are the focus of this article.[14,15,18,19]

The main objective of this research was to develop two mathematical models for the stripping section of an industrial EPDM rubber production process. The steady-state models provide accurate predictions of concentrations of residual solvent and comonomers in the rubber particles that exit each vessel in a train of three or four stripping vessels. The models developed in this article do not require the restrictive assumptions used by Cozewith and Matthews who assumed similar operating conditions. Both models account for diffusion-limited mass transfer from the crumb particles as a function of stripper operating conditions and particle size. The first model focuses on a single particle that moves from tank to tank and the second more complicated model considers all of the EPDM particles within the stripping vessels and assumes a CFST residence time distribution for the tanks, which have different mean residence times. The models are simple enough to use online to provide information for operators and plant engineers.

Background Information

Diffusivities D_j for small molecules (i.e., $j = C6$ for hexane and $j =$ ENB for ENB comonomer) within EPDM rubber

ENB **DCPD**

Figure 2. Structure of diene comonomers used in industrial EPDM.[11]

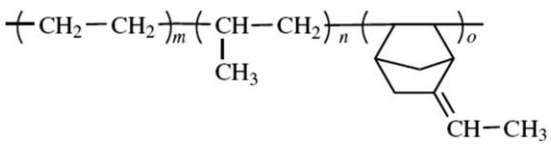

Figure 3. EPDM polymer structure with ENB as the diene comonomer.[11]

Note that the various monomers are arranged randomly in the EPDM rubber.

are important parameters that influences the rate at which stripping occurs. Diffusivities for hexane and ENB were determined by placing a flat sheet (plaque) of EPDM rubber on a scale and contacting the upper surface of the plaque with a nitrogen mixture having a controlled partial pressure of hexane and ENB (as shown in Figure 5). As the plaque is thin compared with its length and width, the diffusion of the small molecules within the plaque can be modeled using the partial differential equation (PDE)[19]

$$\frac{\partial m_j}{\partial t} = D_j \frac{\partial^2 m_j}{\partial x^2} \tag{1a}$$

with the following boundary and initial conditions

$$\frac{\partial m_j}{\partial x}\Big|_{x=0} = 0 \tag{1b}$$

$$m_j|_{x=L} = m_{j\text{eq}} \tag{1c}$$

$$m_j|_{t=0} = m_{jo} \tag{1d}$$

where m_j is the mass concentration (g/kg) of the small molecule on a (dry basis) in the EPDM. x is the vertical coordinate and L is the thickness of the sample. $m_{j\text{eq}}$ is the concentration of small molecules in the rubber that would be in equilibrium with the gas phase so that

$$m_{j\text{eq}} = \frac{P_j}{H_j} \tag{2}$$

where P_j is the partial pressure of small molecule and H_j is the Henry's law coefficient.

Since the gas concentration (hence $m_{j\text{eq}}$ is constant) after time zero, the analytical solution of Eq. 1 is[20]

$$M_j(t) = \frac{\bar{m}_j(t) - m_{jo}}{m_{j\text{eq}} - m_{jo}} = 1 - \frac{8}{\pi^2} \sum_{n=0}^{\infty} \frac{1}{(2n+1)^2} e^{\left(\frac{-D_j t (2n+1)^2 \pi^2}{4L^2}\right)} \tag{3}$$

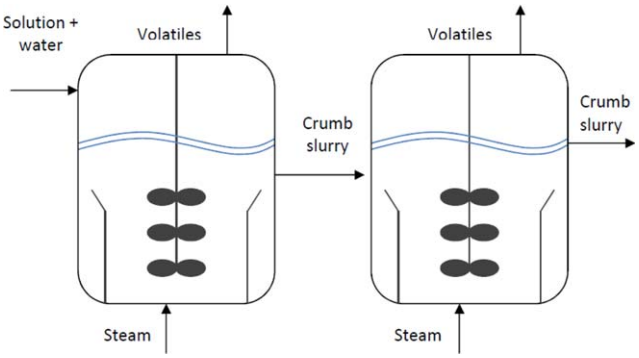

Figure 4. Schematic diagram of a single stripping vessel.

[Color figure can be viewed in the online issue, which is available at wileyonlinelibrary.com.]

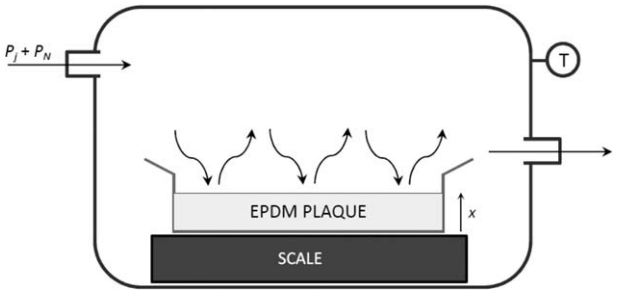

Figure 5. A schematic diagram of the gravimetric testing apparatus (not to scale) at constant temperature, *T* and constant monomer or solvent partial pressure, P_j.

where $M_j(t)$ is the fraction of the way to equilibrium, t is the time that the plaque has been exposed to the imposed gas concentration, and $\bar{m}_j$ is the average concentration of small molecules within the plaque. If the plaque contains only a single small molecule, changes in the measured mass of the plaque over time can be used to determine $M_j(t)$ and to estimate the diffusivity coefficient in Eq. 3.

The effective radius for the EPDM crumb was determined using the following PDE which describes the diffusion from spherical EPDM particle with radius R[15]

$$\frac{\partial m_j}{\partial t} = -D_j\left(\frac{2}{r}\frac{\partial m_j}{\partial r} + \frac{\partial^2 m_j}{\partial r^2}\right) \tag{4a}$$

The following initial and boundary conditions apply during the experiments conducted to estimate R because the particle have initial concentration m_{j0} and the particle surfaces come in contact with a gas phase with partial pressure P_j

$$m_j(r,0) = m_{j0} \tag{4b}$$

$$\frac{\partial m_j}{\partial r}\Big|_{r=0} = 0 \tag{4c}$$

$$m_j(R,t) = m_{j\text{eq}} \tag{4d}$$

where R is the radius of the particles. The analytical solution for Eq. 4 is[20]

$$M_j(t) = \frac{m_j(t) - m_{jo}}{m_{j\text{eq}} - m_{jo}} = 1 - \frac{6}{\pi^2}\sum_{n=1}^{\infty}\frac{e^{\left(-\frac{D_j n^2 \pi^2 t}{R^2}\right)}}{n^2} \tag{5}$$

Table 1 contains a list of assumptions that are consistent with using Eq. 4 to predict mass transfer of solvent and comonomers from crumb particles that pass through the series of stirred tanks.

Experimental Determination of Key Physical Properties for Model Development

Values of diffusivities, Henry's law parameters and effective radii are required to predict stripping performance. A series of gravimetric experiments were conducted to estimate diffusion coefficients and Henry's law constants for hexane and ENB in EPDM rubber. The characteristic diffusion radius of EPDM crumb particles for one EPDM grade was also determined. Gas-phase partial pressures of hexane and ENB in these experiments ranged from 0 to 90 kPa as these are the partial pressures that are typically present in the headspace in industrial stripping tanks. Experiments were repeated using five selected temperatures between 90 and 140°C. A schematic diagram of the apparatus used for the gravimetric experiments is provided in Figure 5.

When preparing plaques for the gravimetric experiments, approximately 2.5 g of EPDM rubber was pressed flat using a heated hydraulic press resulting in a sheet with a thickness of ~1 mm. The mass of the plaque and its thickness, L, were measured. Samples were placed in a tray that hangs from a scale within a temperature-controlled, double-walled glass chamber. The gravimetric testing apparatus included a computer control system that regulated experimental conditions and collected temperature, pressure, and mass data. Temperature was controlled using ethylene glycol, which circulated between the two glass walls. Nitrogen gas and the hexane and ENB were mixed externally, and then flowed into the headspace of the glass vessel to contact the sample. The flows of nitrogen and hexane or ENB were selected to achieve the desired partial pressures. At the beginning of each experiment, only nitrogen gas was fed to the apparatus to ensure that the rubber sample would start from an equilibrium condition free from hexane and ENB. After reaching the initial mass and temperature equilibrium (i.e., after approximately 2 h), flow of either hexane or ENB was initiated to achieve the desired partial pressure for the first step in a series of step tests. After the sample reached a constant mass, the small-molecule flow rate was adjusted to a second

Table 1. Assumptions for the PDE Model (Eq. 4) to Predict Mass Transfer of Small Molecules from Crumb Particles

1	The only components present in the system include: water, EPDM crumb, hexane, and ENB. All other components are negligible in quantity and can be ignored in the model.
2	All resistances to mass transfer are in the solid crumb phase. Mass-transfer resistances in the gas phase and in the water are negligible.
3	The particle-size distribution of the crumb is sufficiently narrow so that the average particle size is used in the model and the particles that make up the crumbs are nearly spherical so that the effective radius R can be used to model the diffusion of small molecules in the crumb.
4	Hexane and ENB in the EPDM crumb begin to be desorbed out of the crumb immediately on entering the tank. Further desorption occurs in the stripping vessels that follow and no desorption occurs in the pipes between tanks, due to the short residence time in the pipes.
5	Heat transfer is typically much faster than mass transfer of small molecules in polymer particles so that the temperature throughout the crumb particle can be assumed to reach the water (and headspace) temperature instantaneously on entering a new stripping tank.
6	The gas headspace behaves as an ideal gas and the headspace concentrations are at steady state.
7	The particles entering the first tank in the stripping section have uniform radial distributions of volatile components.
8	At the particle surface, the volatiles dissolved in the polymer are in equilibrium with the vapour phase.
9	Concentrations of small molecules in the particle are sufficiently low so that Henry's law applies between the particle surface and the gas phase.
10	Henry's law coefficients and diffusion coefficients depend only on temperature and not on the type of EPDM or on the concentrations of small molecules, so that $m_{j,\text{eq}}$ for each tank can be computed from the corresponding stripper temperature and gas-phase partial pressures.
11	The effective particle radius R remains constant as the small molecules are removed.

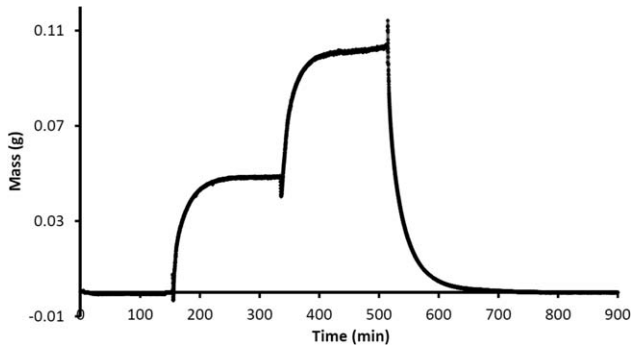

Figure 6. A sample set of data from gravimetric experiments.

and sometimes a third level. After step-change tests were completed, only nitrogen was fed to the chamber, resulting in desorption of the small molecule from the polymer sample. The gravimetric test ended when the final equilibrium free from hexane and ENB was reached. The measured response of the mass reading for a dynamic test with hexane is shown in Figure 6.

Henry's law constants for hexane and ENB were determined from steady-state portions of the data from the step-test experiments using

$$H_j = \frac{P_j}{m_{\text{eq},j}} \tag{6}$$

When several values of H_j were available from the same dynamic experiment, an average value was reported. Diffusivity values for hexane and ENB were determined from the dynamic portions of the data. The fraction of the way to equilibrium $M_j(t)$ was calculated for each data point. Equation 3 was used to fit the corresponding diffusivity via nonlinear regression. The infinite sum in Eq. 3 was evaluated using only the terms from $n = 0$ to $n = 6$, because additional terms had negligible influence on predictions of $M_j(t)$.

Similar dynamic experiments were then conducted using approximately 2.5 g of rubber particles in place of the plaque, to estimate the equivalent radius R. Fitted values of diffusivities from the plaque experiments were used in Eq. 5 to determine R via nonlinear regression.

Solubility and Diffusivity Results

Over the range of experimental conditions used in the experiments, there was no significant effect of hexane or ENB concentration on the estimated Henry's law coefficients and diffusivities. This result is somewhat surprising because Cozewith and Matthews found that the diffusivity of hexane depends on hexane concentration in ethylene propylene rubber (EPR).[15,18,19] Details of the raw data and the corresponding analysis are provided by Francoeur.[21]

The following Arrhenius relationships were used to correlate the effect of temperature on the Henry's law constants and diffusivities

$$H_j(T) = H_{j,\text{ref}} \quad \exp\left(\alpha_j\left(\frac{1}{T} - \frac{1}{T_{\text{ref}}}\right)\right) \tag{7}$$

$$D_j(T) = D_{j,\text{ref}} \quad \exp\left(\beta_j\left(\frac{1}{T} - \frac{1}{T_{\text{ref}}}\right)\right) \tag{8}$$

The reference temperature, T_{ref}, was set at 381.15 K. Table 2 shows the resulting estimated values for the Henry's law constant and diffusivity at 381.15 K ($H_{j,\text{ref}}$ and $D_{j,\text{ref}}$) for hexane and ENB. Approximately 95% confidence intervals are also shown. Note that the diffusivity for ENB at 381.15 K is lower than the diffusivity for hexane, as expected because ENB molecules are considerably larger. The values in Table 2 were fitted using data from two different grades of commercial EPDM. There was no significant difference in the Henry's law coefficients or diffusivities obtained using the two different grades of rubber. Estimates for the equivalent radius from several step tests are summarized in Table 3 for crumb obtained from a commercial EPDM process. The range of values for the characteristic radius is consistent with visual observations of the crumb particles.

At 378.15 K, Eq. 8 predicts a value of D_{C6} of 3.2×10^{-10} m^2/s which is consistent with values of 2.4×10^{-10} m^2/s, and 4.6×10^{-10} m^2/s reported by Mathews et al.[19] for hexane concentration of 5 and 10 wt % of hexane in the EPR particles. Matthews et al.[19] reported the effective radius of approximately 1 mm for EPDM crumb particles obtained from an industrial EPR process which is consistent with approximately 1.355 mm for the EPDM particles for current experiments.

Single-Particle Multiple-Tank Model Development

Consider a single particle that spends time t_1 in one well-mixed stripping vessel and then spends time t_2 in a second stripping vessel with different operating conditions than the first. The average concentration of hexane in the particle leaving the first tank, $m_{C6,1}(t_1)$, can be determined using Eq. 5, given the initial uniform concentration $m_{C6,0}$, the diffusion coefficient $D_{C6,1}$ and equilibrium concentration $m_{\text{eq}C6,1}$ that match the operating conditions in the first tank. The crumb particle then enters the second tank where different values of D_{C6} and $m_{\text{eq}C6}$ apply. The PDE in Eq. 4 can be used to find a rigorous solution for $m_{C6,2}$ if the boundary conditions at the surface of the particle are changed abruptly from $m_{\text{eq}C6,1}$ to $m_{\text{eq}C6,2}$ at t_1 hours and the diffusivity is changed from $D_{C6,1}$ to $D_{C6,2}$ to reflect the different temperature in Tank 2.

Table 2. Henry's Law Constant and Diffusivity Parameters for Hexane and ENB in EPDM Rubber Estimated from Gravimetric Experiments Conducted between 363.15 and 413.15 K

	Parameter	Units	Estimates ±95% Confidence Intervals
Henry's law constant for hexane in EPDM	$H_{C6,\text{ref}}$	kPa-kg/g	1.535 ± 0.074
	α_{C6}	K	3503.6 ± 419
Henry's law constant for ENB in EPDM	$H_{\text{ENB,ref}}$	kPa-kg/g	0.1013 ± 0.0179
	α_{ENB}	K	4719 ± 1314
Diffusivity of hexane in EPDM	$D_{C6,\text{ref}}$	m^2/s	$3.42 \times 10^{-10} \pm 5.7 \times 10^{-11}$
	β_{C6}	K	2800 ± 1373
Diffusivity of ENB in EPDM	$D_{\text{ENB,ref}}$	m^2/s	$1.47 \times 10^{-10} \pm 1.6 \times 10^{-11}$
	β_{ENB}	K	2922 ± 817

Table 3. Characteristic Radii Determined Using a Diffusivity Value of 5.94×10^{-10} m^2/s for Hexane Diffusion into EPDM Grade 1 at 381.15 K

Case	Characteristic Radius (mm)
Step change: 0–5.0 kPa	0.711
Step change: 5.0–50.0 kPa	1.517
Step change: 50.0–86.0 kPa	1.319
Step change: 86.0–0 kPa	2.145
Lumped estimate	1.355

Note that Eq. 5 applies to individual particles exiting the first tank, but is not appropriate for determining the average concentration in particles leaving the second and subsequent tanks because particles that leave the second tank have a radial concentration profile (with higher concentrations in the center of the particles than at the edge). Use of Eq. 5 requires a uniform concentration throughout the particle when it enters the tank. However, the PDE in Eq. 4 can be used to predict average concentrations in individual particles as they pass through several tanks if the boundary condition at the particle surface is changed at appropriate times during the simulation to reflect the conditions in the next tank. The overall concentrations of small molecules in the EPDM rubber that leave the final tank could theoretically be predicted by solving this PDE model repeatedly for a large number of particles that spend different times in different tanks and then computing an appropriate average.

A simplified algebraic method, shown schematically using the dashed lines in Figure 7, is proposed to account for the radial hexane gradient in the crumb leaving the first vessel in an approximate fashion. Imagine that a hypothetical particle with initial concentration $m_{C6,0}$ is placed directly into Tank 2 for a period of time t'_2 rather than spending time t_1 in Tank 1. We define t'_2 as the amount of time that the hypothetical particle would need to spend in Tank 2 to achieve the same average hexane concentration $m_{C6,1}$, which is the same concentration as in the real particle leaving the first vessel. From Eq. 5

$$\frac{m_{C6,1}(t_1)-m_{C6,0}}{m_{\mathrm{eq}\,C6,2}-m_{C6,0}}=1-\frac{6}{\pi^2}\sum_{n=1}^{\infty}\frac{e^{\left(-\frac{D_{C6,2}n^2\pi^2t'_2}{R^2}\right)}}{n^2} \tag{9}$$

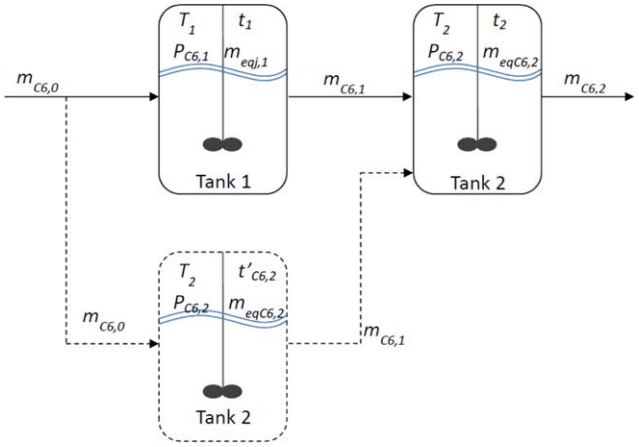

Figure 7. Schematic diagram indicating the methodology of the simple equivalent-time model.

[Color figure can be viewed in the online issue, which is available at wileyonlinelibrary.com.]

Table 4. Simple Equivalent-Time Model Method for Calculating the Average Hexane Concentration Exiting Four Stripping Vessels in Series

1	Use the temperatures and hexane partial pressures in the four tanks to determine the equilibrium hexane concentrations (i.e., $m_{\mathrm{eq}C6,1}$, $m_{\mathrm{eq}C6,2}$, $m_{\mathrm{eq}C6,3}$, and $m_{\mathrm{eq}C6,4}$) using Eqs. 6 and 7. Use the temperatures in the four tanks and Eq. 8 to determine hexane diffusivity values (i.e., $D_{C6,1}$, $D_{C6,2}$, $D_{C6,3}$, and $D_{C6,4}$).
2	Use $m_{\mathrm{eq}C6,1}$, $D_{C6,1}$, t_1, $m_{C6,0}$, and Eq. 5 to determine $m_{C6,1}$, the average concentration of hexane in the particle when it exits Tank 1.
3	Determine the equivalent amount of time $t'_{C6,2}$ that a particle with initial concentration $m_{C6,0}$ would need to spend in Tank 2 with $m_{\mathrm{eq}C6,2}$ and $D_{C6,2}$ to reach a hexane concentration of $m_{C6,1}$ using Eq. 9.
4	Compute $m_{C6,2}$, the approximate concentration of the particle after it leaves Tank 2, using $m_{\mathrm{eq}C6,2}$, $D_{C6,2}$, and a total time of $t = t'_{C6,2} + t_2$ in Eq. 11.
5	Determine the equivalent amount of time $t\prime_{C6,3}$ that a particle with initial concentration $m_{C6,0}$ would need to spend in Tank 3 with $m_{\mathrm{eq}C6,3}$ and $D_{C6,3}$ to reach a hexane concentration of $m_{C6,2}$ using Eq. 9.
6	Compute $m_{C6,3}$, the approximate concentration of the particle after it leaves Tank 3, using $m_{\mathrm{eq}C6,3}$, $D_{C6,3}$, and a total time of $t=t'_{C6,3}+t_3$ in Eq. 11.
7	Determine the equivalent amount of time $t\prime_{C6,4}$ that a particle with initial concentration $m_{C6,0}$ would need to spend in Tank 4 with $m_{\mathrm{eq}C6,4}$ and $D_{C6,4}$ to reach a hexane concentration of $m_{C6,3}$ using Eq. 9.
8	Compute $m_{C6,4}$, the approximate concentration of the particle after it leaves Tank 4, using $m_{\mathrm{eq}C6,4}$, $D_{C6,4}$, and a total time of $t=t'_{C6,4}+t_4$ in Eq. 11.

Equation 9 can be solved to obtain t'_2, given the average concentration $m_{C6,1}(t_1)$ obtained for the real particle from Eq. 5

$$\frac{m_{C6,1}(t_1)-m_{C6,0}}{m_{\mathrm{eq}\,C6,1}-m_{C6,0}}=1-\frac{6}{\pi^2}\sum_{n=1}^{\infty}\frac{e^{\left(-\frac{D_{C6,1}n^2\pi^2t_1}{R^2}\right)}}{n^2} \tag{10}$$

It is reasonable to assume that if the hypothetical particle would spend a total time of t'_2+t_2 in Tank 2, it would have a similar final average hexane concentration as the real particle, which spends t_1 in Tank 1 and t_2 in Tank 2. As a result, the concentration in the real particle leaving Tank 2 can be estimated from

$$\frac{m_{C6,2}(t_1+t_2)-m_{C6,0}}{m_{\mathrm{eq}\,C6,2}-m_{C6,0}}\cong 1-\frac{6}{\pi^2}\sum_{n=1}^{\infty}\frac{e^{\left(-\frac{D_{C6,2}n^2\pi^2(t'_2+t_2)}{R^2}\right)}}{n^2} \tag{11}$$

The error in this calculation results from the fact that the radial profile of hexane in the real particle leaving Tank 1 may be slightly different than the radial profile of hexane in the hypothetical particle that spends t'_2 in the second tank. In Table 4, this equivalent-time methodology is extended to predict the average concentration of hexane and ENB in a particle that has passed through four of tanks in series. The error obtained when Eq. 11 is used, is investigated in Figure 8. In this figure, the solutions from the simplified equivalent-time model are compared with the rigorous PDE solution for a particle with $R = 1.355$ mm and $m_{C6,0} = 350$ g/kg and at typical operating conditions. These simulation results show that the simple model predictions are similar to predictions from the PDE model for a range of industrially relevant values of t_1 and t_2. As expected, long t_2 values that are greater

Table 5. Discretized Bin Method for Calculating the Average Concentration of Small Molecules *j* in Particles Leaving the First Tank

1	Calculate the average residence time τ_1 time for particles in Tank 1.
2	Using this table, make an array of time bins for the total population of particles experiencing residence times from 0 to $12\tau_1$, keeping track of the times associated with the left and right edge of each bin (i.e., t_{b1L} and t_{b1R} for all 48 values of b1).
3	Calculate the average time, t_{b1}, associated with each bin using Eq. 14.
4	Calculate the fraction of particles, ϕ_{b1}, associated with each bin using t_{b1L}, t_{b1R}, τ_1, and Eq. 15.
5	Use $m_{\mathrm{eq}j,1}$, $D_{j,1}$, t_{b1}, and Eq. 5 to calculate $m_{b1,j,1}$ for each bin and for each species.
6	Use Eq. 16, $m_{b1,j,1}$ and ϕ_{b1} for all bins to calculate $\bar{m}_{j,1}$ for each species.

than ~0.75 h result in the hexane in the crumb particles reaching equilibrium in Tank 2, independent of how long they spent in Tank 1. Numerical solutions for the PDE model were obtained using the *pdepe* solver in Matlab™ with convergence criteria set to ensure a relative error <0.1% or an absolute error $<1 \times 10^{-5}$ g/kg. The average concentration within the particle was calculated by numerical integration.[21] The equivalent-time model gives good predictions of average concentrations of both hexane and ENB for particles passing through multiple tanks with operating conditions that correspond to typical industrial conditions.[21] One difficulty with using the equivalent-time approach is that implicitly solving Eq. 9 to obtain t_2' requires an iterative method (e.g., Newton's method). The main shortcoming of the equivalent-time model is that it only applies to individual particles rather than to a mixture of particles with a residence time distribution. Calculating $\bar{m}_{C6,2}$ using representative particles that spend the average residence times τ_1 and τ_2 in Tanks 1 and 2 may result in underprediction of the hexane content in the overall EPDM leaving Tank 2. The reason for this underprediction is that particles that spend times less than τ_1 and τ_2 in the tanks may have hexane concentrations that are substantially higher than this estimated value of $\bar{m}_{C6,2}$. Particles that spend longer than τ_1 and τ_2 in the tanks may have hexane concentrations that are only slightly lower than this estimate for $\bar{m}_{C6,2}$.

CFST-Distribution Multiple-Tank Model Development

This section describes a method to predict the average concentration ($\bar{m}_{j,i}$) of species *j* in a large sample of particles that leave tank *i*, assuming that the particles in the various tanks follow residence time distribution. The residence time distribution in each tank depends on its average residence time τ_i according to[22,23]

$$E(t) = \frac{1}{\tau_i} e^{-\left(\frac{t}{\tau_i}\right)} \tag{12}$$

To obtain the average concentration of small molecule (hexane or ENB) *j* in crumb particles exiting a single CFST, Eq. 5 can be integrated over the residence time distribution for the crumb particles giving[15]

$$\frac{\bar{m}_j(t_1) - m_{jo}}{m_{j\mathrm{eq}} - m_{jo}} = 1 - \frac{6}{\pi^2} \sum_{n=1}^{\infty} 1/\left(\frac{n^4 \pi^2 D_j \tau_1}{R^2} + n^2 \right) \tag{13}$$

Consider a series of four CFSTs where the situation becomes more complicated, requiring numerical integration over the range of possible values for t_1, t_2, t_3, and t_4 as well as calculation of the corresponding equivalent-times t_2', t_3', and t_4' if the equivalent-time method from Table 4 is applied to the individual particles that move from tank to tank. Analytical integration is not possible because solving Eq. 9 to obtain t_2' requires an iterative method. The proposed tanks-in-series model developed here uses numerical integration, which requires discretizing the residence time distribution for each tank using particle bins. The bins are selected so that particles in the same bin have similar hexane or ENB concentrations and spend approximately the same amounts of time in the various tanks. As a result, Eq. 5 can be used to predict the appropriate hexane concentration for each bin in the first tank. Concentrations for particles in each bin can then be combined to compute the overall average concentration (i.e., $\bar{m}_{j,1}$) for the EPDM leaving Tank 1.

It was determined that using 48 discrete time bins within the time range from 0 to $12\tau_i$ was sufficient to accurately calculate the resulting $\bar{m}_{j,i}$ values for the various tanks. To improve the accuracy of the calculations, bins were not evenly spaced in time; wider spacing was used for longer times where particles tended to have lower concentrations. Details are provided by Francoeur.[21] The representative time corresponding to particles in a particular bin was assigned as the average value

$$t_{bi} = \frac{t_{biL} + t_{biR}}{2} \tag{14}$$

where t_{biL} corresponds to the time at the left edge of the *b*th bin in tank *i* and t_{biR} corresponds to the time at the right edge of the *b*th bin. Assuming a CFST residence time distribution, the fraction of particles that spend between t_{b1L} and t_{b1R} in the first tank is

$$\phi_{b1} = e^{-\left(\frac{t_{b1L}}{\tau_1}\right)} - e^{-\left(\frac{t_{b1R}}{\tau_1}\right)} \tag{15}$$

so that the overall average concentration of species *j* exiting the first tank is

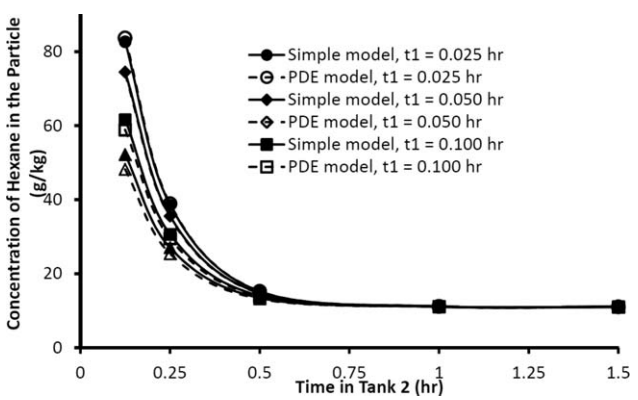

Figure 8. Resulting hexane concentrations remaining in the spherical EPDM particle after spending various times in Tank 1 and Tank 2.

Table 6. Equations Required for Determining the Headspace Concentrations

Equation	Number
$P_W^{\text{sat}} = 10 \times e^{\left(16.3872 - \left(3885.7/(T+230.17)\right)\right)}$	(17)
$y_W = \frac{P_W^{\text{sat}}}{P}$	(18)
$\gamma_i = \frac{1 - y_{W,i}}{\sum_j \left(F_{\text{dif}\,j,i} + F_{\text{pre}\,j,i}\right)}$	(19)
$y_{j,i} = \gamma_i \left(F_{\text{dif}\,j,i} + F_{\text{pre}\,j,i}\right)$	(20)
$F_{\text{dif}\,j,i} = F_{\text{in}\,j,i} - F_{\text{out}\,j,i}$	(21)
$F_{\text{in}\,j,i} = \left(\frac{\bar{m}_{j,i-1}\ F_{\text{crumb}}}{100}\right)/\text{MW}_j$	(22)
$F_{\text{out}\,j,i} = \left(\frac{\bar{m}_{j,i}\ F_{\text{crumb}}}{100}\right)/\text{MW}_j$	(23)
$m_{\text{eq}\,j,i} = \frac{P_i\ y_{j,i}}{H_{j,i}}$	(24)

$$\bar{m}_{j,1} = \sum_{b1=1}^{48} \left(\phi_{b1} m_{b1,j,1}\right) \tag{16}$$

where $m_{b1,j,1}$ is the concentration of species j for the crumb in the $b1$th bin. Each value of $m_{b1,j,1}$ is calculated using $m_{\text{eq}j,1}$, $D_{j,1}$, t_{b1}, and Eq. 5. Table 5 summarizes the steps and equations used to calculate average species concentrations exiting Tank 1 (i.e., $\bar{m}_{j,1}$ values) using the discretized bin method. Calculation of the compositions of the hexane and ENB for the crumb particles in each bin requires knowledge of the headspace partial pressures, which are calculated from the headspace mole fractions and the measured overall pressures in the stripping tanks. The headspace compositions are not measured, but can be calculated using the equations in Table 6 and the iterative method described in Table 7.

To extend the discretized bin method for a two-tank model, a two-dimensional (2-D) array of bins is used. Each element in the array corresponds to the fraction of particles that spends between t_{b1L} and t_{b1R} in Tank 1 and between t_{b2L} and t_{b2R} in Tank 2. To calculate the fraction of particles in each bin within the 2-D array, Eq. 12 is used first to calculate $E(t_{b1L})$, $E(t_{b1R})$, $E(t_{b2L})$, and $E(t_{b2R})$. Next, the 2-D trapezoidal rule is used to calculate the fraction of particles in each element of the 2-D array

$$\phi_{b1,b2} = (t_{b1R} - t_{b1L})(t_{b2R} - t_{b2L}) \frac{E(t_{b1R}) + E(t_{b1L}) + E(t_{b2R}) + E(t_{b2L})}{4} \tag{25}$$

Analogous to Eq. 16, the average concentration for each species in the crumb leaving Tank 2 is

$$\bar{m}_{j,2} = \sum_{b2=1}^{48} \sum_{b1=1}^{48} \left(\phi_{b1,b2} m_{b1,b2,j,2}\right) \tag{26}$$

where $m_{b1,b2,j,2}$ is the concentration of species j within the crumb corresponding to bin $b1$ in Tank 1 and bin $b2$ in Tank 2. $m_{b1,b2,j,2}$ is calculated using the equivalent-time approach described in Table 4. Table 8 summarizes this method for computing $\bar{m}_{j,2}$. Extending this discretized bin to additional tanks would require $48^3 = 110{,}592$ separate bins for particles exiting the third tank and $48^4 = 5{,}308{,}416$ separate bins for particles exiting the fourth tank. To prevent this bin dimensionality explosion, an additional assumption was made, wherein particles from multiple bins are lumped together. Particles in the 48×48 bins exiting Tank 2 are lumped into a single array of 48 bins. This lumping the 2-D array of $m_{b1,b2,j,2}$ values into a 1-D array using equivalent-time ideas is described in Table 9. After method in Table 9 has been used to determine the times for the bin edges $t_{b2'L}$ and $t_{b2'R}$, the fraction of the particles in each bin $\phi_{b2'}$ and the average concentration in each bin $m_{b2',j,2}$, the methodology in Table 8 easily used to calculate the resulting $m_{b2',b3,j,3}$ and $\bar{m}_{j,3}$ values. Similar lumping of bins in Tank 3 is used to compute for industrial situations involving four tanks in series.

Table 7. Iterative Method Used for Calculating the Gaseous Headspace Concentrations of Each Species in Tank *i* in a Series of Stripping Vessels

1	Compute $y_{W,i}$ using Eqs. 6 and 7, and assume initial molar fractions for other species in the headspace (i.e., $y_{C6,i,\text{guess}}$, $y_{\text{ENB},i,\text{guess}}$) so that the mole fractions add to one.
2	Use P_i, $y_{C6,i,\text{guess}}$, $y_{\text{ENB},i,\text{guess}}$, $H_{C6,i}$, $H_{\text{ENB},i}$, and Eq. 24 to determine $m_{\text{eq}C6,i}$ and $m_{\text{eqENB},i}$.
3	Use $m_{\text{eq}j,i}$, $D_{j,i}$, t, $\bar{m}_{j,i-1}$, and Table 4 to determine $\bar{m}_{j,i}$ for each species.
4	Compute the mass flow rate of each species entering the tank within the crumb (i.e., $F_{\text{in}C6,i}$ and $F_{\text{inENB},i}$) using $\bar{m}_{C6,i-1}$, $\bar{m}_{\text{ENB},i-1}$, F_{crumb}, MW_{C6}, MW_{ENB}, and Eq. 24. Also, compute the mass flow rate of each species exiting the tank within the crumb (i.e., $F_{\text{out}C6,i}$, $F_{\text{outENB},i}$) using $\bar{m}_{C6,i}$, $\bar{m}_{\text{ENB},i}$, and Eq. 23.
5	Using $F_{\text{in}C6,i}$, $F_{\text{inENB},i}$, $F_{\text{out}C6,i}$, $F_{\text{outENB},i}$, and the mass balance Eq. 23, determine the flow rate of each species diffusing out of the crumb and into the gas headspace (i.e., $F_{\text{dif}C6,i}$, $F_{\text{difENB},i}$).
6	Using $y_{W,i}$, $F_{\text{dif}C6,i}$, $F_{\text{difENB},i}$, the inlet gaseous flow rates for each species (i.e., $F_{\text{pre}C6,i}$, $F_{\text{preENB},i}$) and the material balance Eq. 21, determine Υ_i.
7	Use γ_i, $F_{\text{dif}C6,i}$, $F_{\text{difENB},i}$, $F_{\text{pre}C6,i}$, $F_{\text{preENB},i}$, and Eq. 22 to determine new headspace concentrations: $y_{C6,i,\text{new}}$, $y_{\text{ENB},i,\text{new}}$.

Parameter Tuning

Model parameters were estimated so that predicted concentrations in the crumb exiting each stripping tank match industrial data collected from three EPDM processes, one

Table 8. Discretized Bin Method for Calculating the Average Concentration of Species *j* in Particles Exiting the Second Tank

1	Determine the average residence time τ_1 time for particles in Tank 1. Use Table 5 to determine t_{b1L}, t_{b1R} and use Eq. 14 to calculate t_{b1}. Next use the equation in Table 7 and the method in Table 8 to determine $y_{j,1}$, $m_{b1,j,1}$ and $\bar{m}_{j,1}$ for each species and for each bin in Tank 1. Use Eq. 12 and $\tau = \tau_1$ to determine $E(t_{b1L})$, $E(t_{b1R})$ for each bin in Tank 1.
2	Calculate the average residence time τ_2 time for particles in Tank 2. Use Table 5, Eq. 14 and $\tau = \tau_2$ to determine t_{b2L}, t_{b2R}, t_{b2}. Use Eq. 12 to determine $E(t_{b2L})$ and $E(t_{b2R})$ for each bin in Tank 2. Use Eq. 12 and $\tau = \tau_1$ to determine $E(t_{b1L})$, $E(t_{b1R})$ for each bin in Tank 1.
3	Calculate the fraction of particles, $\varphi_{b1,b2}$, associated with each element in the 2-D array using $E(t_{b1L})$, $E(t_{b1R})$, $E(t_{b2L})$, $E(t_{b2R})$ and Eq. 25.
4	Perform steps 1–3 from Table 4 to determine the equivalent-time $t'_{2b1,j}$ for each bin in Tank 1, for each species, using $m_{\text{eq}j,2}$, $m_{b1,j,1}$, $D_{j,2,}$ T_2, and $m_{j,0}$.
5	Perform step 4 from Table 4 for each element in the 2-D array of bins to determine $m_{b1,b2,j,2}$ for each element, for each species, using $t_{b1,b2,j,2} = t'_{2b1,j} + t_{b2}$, $m_{\text{eq}j,2}$, $D_{j,2,}$ T_2, and $m_{j,0}$.
6	Use Eq. 26, $m_{b1,b2,j,2}$ and $\phi_{b1,b2}$ for all bins to obtain $\bar{m}_{j,2}$ for each species.

Table 9. Lumping Method Used to Convert a 2-D Matrix of $m_{b1,b2,j,2}$ Values into a 1-D Array of $m_{b2\prime,j,2}$ Values

1	Determine the average residence time τ_1 time for particles in Tank 1. Use Eq. 5, $m_{eqj,1}$, $D_{j,1}$, $m_{j,0}$, and $t = \tau_1$ to determine the concentration of species j in a typical particle spending τ_1 time in Tank 1. Perform this calculation for each species.
2	Determine the equivalent amount of time $\tau'_{j,2}$ that a particle with initial concentration $m_{j,0}$ would need to spend in Tank 2 with $m_{eqj,2}$ and $D_{j,2}$ to reach a concentration of $m_{j,1}$ using Eq. 9. Perform this calculation for each species.
3	Determine the minimum of $\tau'_{C6,2}$ and $\tau'_{ENB,2}$ (i.e., $\tau'_{min,2}$).
4	Perform steps 1 and 3 using $\tau = \tau_2 + \tau_{min,2}$, and use Table 6 to determine $t_{b2'L}$, $t_{b2'R}$, $t_{b2'}$, $E(t_{b2'L})$, and $E(t_{b2'R})$ for each bin.
5	For each of the new equivalent-time bins in Tank 2, search for all values of $t_{b1,b2,j,2}$ that satisfy: $t_{b2'L} < t_{b1,b2,j} < t_{b2'R}$. Sum the fractional concentrations of species j in the crumb (i.e., $m_{b1,b2,j,2} \times \varphi_{b1,b2}$) for all of the bins lumped into each $t_{b2'}$ bin to estimate $m_{b2',j,2}$ for each of the lumped bins. Also, sum the fraction $\varphi_{b1,b2}$ for bins that are lumped together to obtain $\phi_{b2'}$, the fraction of the overall crumbs in the lumped bin.

with three tanks in series and two with four tanks in series.[21] Steady-state process operating conditions and crumb concentrations were collected on 14 different days from the three-tank process and five and six different days, respectively, from the two four-tank processes. For the three-tank process, outlet crumb concentrations were only available from the second and third tanks due to process sampling limitations. For the four-tank processes, crumb concentration data were available from Tank 2 for some operating conditions, and from Tanks 3 and 4 for all operating conditions. Because the crumb fed to the first tank could not be sampled for any of the processes, predictions from an existing upstream process model developed using Aspen™ were used as inputs to the multitank models.

Table 10 summarizes the adjustable parameters in the three-tank and four-tank models, along with their initial guesses and the uncertainty bounds that were used for deciding which parameters should be estimated from the available data. The first 12 parameters listed in Table 10 are Henry's law and diffusivity parameters. Their initial values and uncertainty ranges were set using the results in Table 2. The next six parameters, $I_{C6,0}$ to $I_{ENB,0B}$ are multiplicative tuning parameters that are used to account for the relatively large uncertainties in inlet concentrations in the crumb (i.e., in $m_{C6,0}$ and $m_{ENB,0}$). For example, the initial guess of $I_{C6,0} = 1.0$ indicates that the input value from the Aspen™ model should be used as is. The lower and upper bounds of 0.4 and 1.6 indicate that there may be up to 60% error in these estimated inlet concentrations. The subscripts A and B refer to four-tank process A and four-tank process B, respectively. Parameters with neither A nor B correspond to the three-tank process. Different multiplicative tuning parameters were used for the different processes, because the Aspen™ model may be better at predicting inlet concentrations in some of the plants compared to the others. The next nine parameters p_1 to p_{34B} are multiplicative pressure tuning parameters for the three-tank process and the two four-tank processes. Note that the 34 subscripts in p_{34A} and p_{34B} are used, because Tanks 3 and 4 in the four-tank processes share a common headspace.

These pressure correction factors are required to solve a problem that encountered while calculating headspace concentrations in some of the tanks using the equations in Table 6. In some situations, the measured pressure in a tank could be lower than the vapor pressure of water calculated using the Antoine equation 17, indicating that there is an error in the measured pressure or temperature or that the liquid water and steam in the stripping tanks may not be in equilibrium. Using a multiplicative tuning factor, p_i, that is slightly greater than 1 can alleviate this computational problem. The next eight parameters, R_1–R_8 are effective radii for the eight different EPDM grades. A relatively narrow uncertainty range is specified for R_3, because it corresponds to the grade used in the experiments described earlier in this article. The remaining 11 tuning parameters in Table 10 are multiplicative factors that were applied to each tank's calculated residence time. Note that parameters Y_1, Y_{3A}, Y_{4A}, Y_{3B}, and Y_{4B} have relatively large uncertainty ranges, based on advice from our industrial sponsor, due to limited knowledge about crumb-flow phenomena in the corresponding tanks.

Table 10. List of Tuning Parameters, Corresponding Initial Guesses and Bounds for Three and Four-Tank Models

Symbol	Units	Initial Guess	Lower Bound	Upper Bound
$H_{C6,ref}$	kPa-kg/g	1.535	1.464	1.609
α_{C6}	K	−3503.6	−3922.4	−3084.7
$H_{ENB,ref}$	kPa-kg/g	0.101	0.086	0.119
α_{ENB}	K	−4719.0	−6033.3	−3404.6
$D_{C6,ref}$	m^2/s	3.42×10^{-10}	2.93×10^{-10}	3.99×10^{-10}
β_{C6}	K	−2800	−4173	−1426
$D_{ENB,ref}$	m^2/s	1.47×10^{-10}	1.33×10^{-10}	1.62×10^{-10}
β_{ENB}	K	−2922	−3739	−2105
$I_{C6,0}$	–	1.00	0.40	1.60
$I_{ENB,0}$	–	1.00	0.40	1.60
$I_{C6,0A}$	–	1.00	0.40	1.60
$I_{ENB,0A}$	–	1.00	0.40	1.60
$I_{C6,0B}$	–	1.00	0.40	1.60
$I_{ENB,0B}$	–	1.00	0.40	1.60
p_1	–	1.00	0.98	1.02
p_2	–	1.00	0.95	1.25
p_3	–	1.00	0.95	1.25
p_{1A}	–	1.00	0.98	1.02
p_{2A}	–	1.00	0.95	1.50
p_{34A}	–	1.30	0.95	1.50
p_{1B}	–	1.00	0.98	1.02
p_{2B}	–	1.00	0.95	1.50
p_{34B}	–	1.10	0.95	1.50
R_1	m	1.355×10^{-3}	0.200×10^{-3}	6.355×10^{-3}
R_2	m	1.355×10^{-3}	0.200×10^{-3}	6.355×10^{-3}
R_3	m	1.355×10^{-3}	3.551×10^{-4}	2.355×10^{-3}
R_4	m	1.355×10^{-3}	0.200×10^{-3}	1.136×10^{-2}
R_5	m	1.355×10^{-3}	0.200×10^{-3}	1.136×10^{-2}
R_6	m	1.355×10^{-3}	0.200×10^{-3}	1.136×10^{-2}
R_7	m	1.355×10^{-3}	0.200×10^{-3}	1.136×10^{-2}
R_8	m	1.355×10^{-3}	0.200×10^{-3}	1.136×10^{-2}
Y_1	–	1.00	0.50	1.50
Y_2	–	1.00	0.95	1.05
Y_3	–	1.00	0.95	1.05
Y_{1A}	–	1.00	0.95	1.05
Y_{2A}	–	1.00	0.95	1.05
Y_{3A}	–	1.00	0.50	1.50
Y_{4A}	–	1.00	0.50	1.50
Y_{1B}	–	1.00	0.95	1.05
Y_{2B}	–	1.00	0.95	1.05
Y_{3B}	–	1.00	0.50	1.50
Y_{4B}	–	1.00	0.50	1.50

Table 11. Uncertainty Associated with Measured Data from the Three-Tank and Four-Tank Processes

Measured Variable	Units	Measurement Uncertainty for Three-Tank Process	Measurement Uncertainty for Four-Tank Processes
$m_{C6,2}$	g/kg	3.1	8.0
$m_{ENB,2}$	g/kg	1.8	0.1
$m_{C6,3}$	g/kg	1.1	3.0
$m_{ENB,3}$	g/kg	0.9	0.9
$m_{C6,4}$	g/kg		1.5
$m_{ENB,4}$	g/kg		0.6

Estimability analysis was used to rank the parameters from the most estimable to least estimable based on their influence on the model predictions, the uncertainties in their initial values, and correlation between parameters.[24,25] The optimal number of parameters to be estimated from the ranked list was selected using a mean square error criterion. This criterion selects the optimal number to estimate (i.e., the 21 parameters in Table 12) so that problems due to overfitting and finest predictions can be prevented.[26–28] Parameters were estimated using the weighted least-squares objective function

$$J = \sum_r \sum_i \sum_j \left(\frac{\mu_{m_{j,i,r}} - \bar{m}_{j,i,r}}{s_{m_{j,i}}} \right)^2 \quad (27)$$

where $\mu_{m_{j,i,r}}$ is the measured concentration of small-molecule j in the crumb leaving the ith tank from the rth dataset and $\bar{m}_{j,i,r}$ is the corresponding predicted concentration. The weighting factors $s_{m_{j,i}}$ in Eq. 27 are uncertainties associated with the different measurements for hexane and ENB, which are shown in Table 11. Note that, in some cases, different measurement uncertainties were assigned for measurements taken from the different processes, based on advice from our industrial sponsor concerning measurement errors and sample collection.

Values for the 21 estimated parameters are shown in Table 12 (estimated using 80 measured values). Note that the 23 parameters that were not estimated were held fixed at the values in Table 10. The parameters in Table 12 are shown in ranked order (i.e., the effective radius R_2 was selected as the most estimable parameter due to its high level of influence on model predictions and its relatively large uncertainty range). All of the estimated parameter values are inside the uncertainty ranges specified in Table 10, except for Y_{4A}, which moved to its upper bound. This result suggests that the crumb residence time in the fourth tank of process B may be substantially longer than the value that was calculated based on the overall tank volume, the water and crumb-flow rates and the expected crumb level in the tank. Details of the parameter selection and estimation procedure are provided by Francoeur.[21]

Table 12. List of the 21 Updated Three- and Four-Tank Parameters

Symbol	Units	Updated Value
R_2	m	1.530×10^{-3}
p_3	–	1.04
R_1	m	7.807×10^{-4}
p_2	–	0.98
$I_{ENB,0}$	–	0.66
p_{34A}	–	1.1573
R_5	m	6.349×10^{-4}
$I_{C6,0A}$	–	0.41
R_4	m	2.212×10^{-4}
$I_{C6,0B}$	–	1.00
$I_{ENB,0B}$	–	1.49
R_8	–	9.245×10^{-4}
R_7	m	1.043×10^{-3}
p_{2B}	–	0.98
p_{34B}	–	1.02
R_6	m	8.78×10^{-3}
$I_{ENB,0A}$	–	1.41
Y_{4A}	–	1.50
$I_{C6,0}$	–	0.85
Y_{3A}	–	0.57
$H_{ENB,ref}$	kPa-kg/g	0.09174

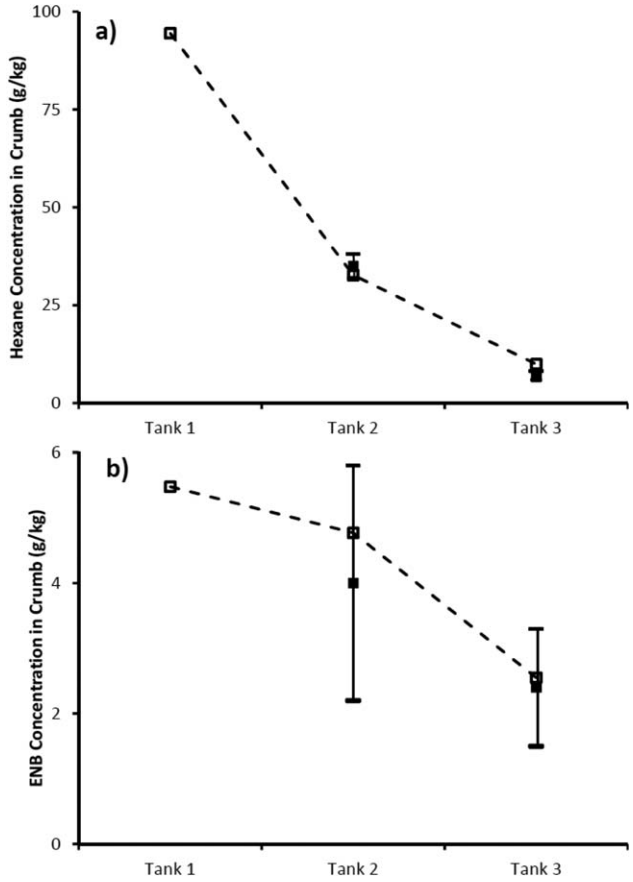

Figure 9. Three-tank simulation results for outlet crumb concentrations (□) compared to measured data (■) for one dataset (a) hexane concentration in crumb $\bar{m}_{C6,i}$ and (b) ENB concentration in crumb $\bar{m}_{ENB,i}$.

Dashed lines between the model predictions are used to guide the eye.

Figures 9 and 10 compare model predictions with typical data from the three- and four-tank processes, respectively, using the estimated parameter values in Table 12. A complete set of comparisons with all of the data is provided by Francoeur.[21] Figures 9 and 10 show that the three- and four-tank models, respectively, were able to provide a good match with the experimental data. As expected, model predictions for hexane and ENB concentrations decreased from tank to tank (see Figures 9 and 10). The model predictions are within error bars on the measurements except for the error bars for hexane in Tank 3 in the three-tank model. The approximate hexane concentration in the crumb that was fed

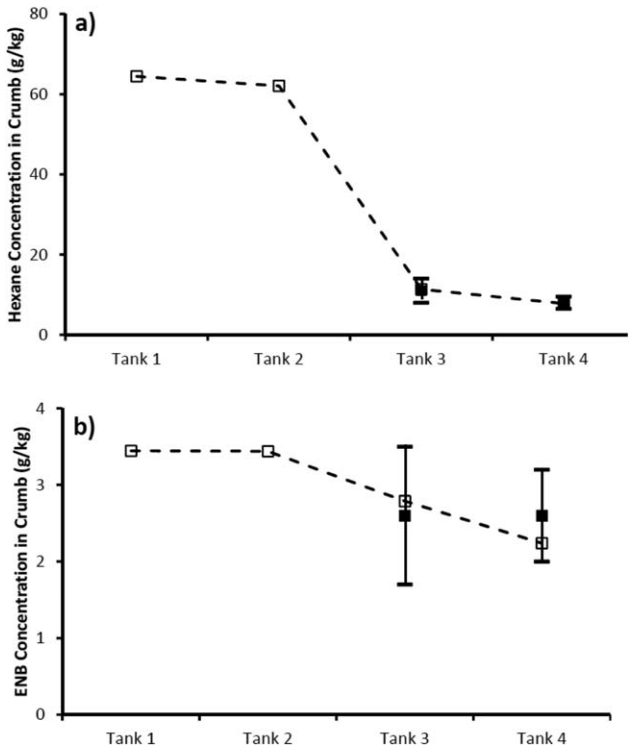

Figure 10. Four-tank simulation results for outlet crumb concentrations (□) compared to measured data (■) for one dataset (a) hexane concentration in crumb $\bar{m}_{C6,i}$ and (b) ENB concentration in crumb $\bar{m}_{ENB,i}$.

Dashed lines between the model predictions are used to guide the eye.

to the three-tank process for the experimental run in Figure 9 was 125.0 g/kg and the inlet ENB concentration was 9.0 g/kg. As a result, in the three-tank process about 92% of the hexane was removed and 72% of the ENB was removed. The large majority of hexane removal occurred in Tank 2 where the concentration of hexane changed from 94.5 to 32.7 g/kg. Most of the ENB removal occurred in Tank 1 where the concentration of ENB fell to 5.48 g/kg. The approximate hexane concentration in the crumb that was fed to the four-tank process for the experimental run in Figure 10 was 80.0 g/kg, and the inlet ENB concentration was 11.2 g/kg. Approximately 90% of the hexane and 80% of the ENB were removed for the experimental run in Figure 10. In the four-tank process, the large majority of hexane and ENB removal was predicted in Tank 1 where the concentrations of hexane and ENB fell to 64.4 and 3.5 g/kg, respectively. The prediction from the model will be helpful to engineers who design and operate the ENB production processes.

Conclusions

A mathematical model for the multitank stripping section of industrial EPDM rubber production processes was developed. Experiments were conducted to determine Henry's law coefficients and diffusivities for hexane solvent and ENB comonomer in EPDM particles. An effective crumb particle radius was also determined for one polymer grade. A simplified algebraic equation model was developed to predict solvent and comonomer concentrations in a single particle that moves from tank to tank, and the predictions from this model provided a good match to predictions from a rigorous PDE model, for the range of industrial conditions that were simulated. This simplified model was then used to develop a more complicated model that accounts for residence time distributions of the crumb particles in CFST stripper in series. Data from three industrial EPDM production plants were used to estimate selected model parameters. The resulting model provides accurate predictions of concentrations of residual hexane and comonomers in the rubber crumb particles that exit each vessel in the train of three or four stripping vessels. The model equations were developed using simplifying assumptions so that numerical solution of complex PDE models is not required. The resulting model equations are simple enough to be solved online or used in process optimization studies to provide information for process engineers.

Acknowledgment

Financial supports provided by LANXESS and MPrime are gratefully acknowledged.

Notation

Abbreviations

ASTM = American Society for Testing and Materials
CFST = Continuous Flow Stirred Tank
DCPD = Dicyclopentadiene
ENB = 5-ethylidene-2-norbornene
EPDM = Ethylene Propylene Diene Monomer
MSE = Mean Squared Error
PDE = Partial Differential Equation

Roman letters

D = diffusivity, m^2/s
$E(t)$ = residence time distribution for CFST
F_{crumb} = mass flow rate of EPDM crumb
F_{dif} = molar flow rate diffusin[11–13,29] g out of the EPDM particles in the tank
F_{in} = molar flow rate entering the tank within the crumb
F_{out} = molar flow rate in the crumb exiting the tank
F_{pre} = molar flow rate flowing into the headspace
F_{crumb} = mass flow rate EPDM crumb through the tank
$F_{dif,j}$ = molar flow rate of species j flowing out of the EPDM particles into the headspace
$F_{pre,j}$ = molar flow rate of species j flowing into the headspace
$F_{in,j,i}$ = molar flow rate of species j entering tank i within the crumb
$F_{out,j,i}$ = molar Flow rate of species j exiting tank i
H = Henry's law constant
$I_{j,0}$ = adjustable factor to tune the inlet concentration of species j in the crumb
J = objective function to minimize parameter estimation
L = thickness of the sample
m = average concentration (g small molecule per kg of polymer free of small molecule)
$\bar{m}$ = average concentration, taking into account the residence time distribution
M = fraction of the way for the small molecule/EPDM system to reach equilibrium
MW = molecular weight
p = adjustable factor to tune the pressure for the three- and four-tank process models
p_{34} = adjustable factor to tune the pressure in Tanks 3 and 4 for the four-tank process model
P = total pressure
P_j = partial pressure for small molecule j
P_W^{sat} = saturation pressure of water, calculated using the Antoine equation
R = particle radius or effective particle radius, m

$s_{m_{j,i}}$ = uncertainty associated with the industrial $m_{j,i}$ data
t = time
t_{bi} = average time spent in tank i by particles in the bith bin
$t_{biL,R}$ = time at the left edge and right edge of the bith bin in tank i
t' = equivalent time
T = temperature
x = diffusion distance in an EPDM plaque
y = mole fractions in gaseous headspace
Y_i = adjustable factor to tune the residence time in tank i

Greek letters

α = activation energy term for the Henry's constant Arrhenius expression
β = activation energy term for the diffusivity-related Arrhenius expression
γ = proportionality factor between molar flow rate and mole fraction in the headspace defined in Eq. 19
$\mu_{m_{j,i,r}}$ = measured concentration of small molecule j in crumb leaving the ith tank from the rth dataset
π = Pi
τ = average residence time
τ' = calculated equivalent average residence time
ϕ = fraction of particles within the specified time bin

Subscripts

0 = indicates the variable at an initial or an inlet condition
A, B = indicated parameters used in the four-tank processes A and B
bi = indicates the time bin number
b'_i = indicates the equivalent-time bin number
$C6$ = used in place of j to indicate hexane
ENB = used in place of j to indicate ENB
eq = indicates a variable at an equilibrium condition
i = indicates the tank number (e.g., 1, 2, 3, 4)
j = indicates the small molecule species (hexane or ENB)
n = indicates the progression through the infinite sum approximation
N = used in place of j to indicate nitrogen
r = indicates the dataset number
ref = indicates the variable at a reference condition
W = used in place of j to indicate water

Literature Cited

1. Kechagia Z, Kammona O, Pladis P, Alexopoulos AH, Kiparissides C. A kinetic investigation of removal of residual monomers from polymer latexes via post-polymerization and nitrogen stripping methods. *Macromol React Eng*. 2011;5:479–489.
2. Araújo P, Sayer C, Giudici R, Poço J. Techniques for reducing residual monomer content in polymers: a review. *Polym Eng Sci*. 2002; 42:1442–1468.
3. Aerts M, Meuldijk J, Kemmere M, Keurentjes J. Residual monomer reduction in polymer latex products by extraction with supercritical carbon dioxide. *Macromol Symp*. 2011;302:297–304.
4. Salazar R, Alvarez D, Ilundain P, Da Cunha L, Barandiaran MJ, Asua JM. Towards the production of green/odorless latexes. *React Funct Polym*. 2004;58:159–164.
5. Salazar R, Ilundain P, Alvarez D, Da Cunha L, Barandiaran MJ, Asua JM. Reduction of the residual monomer and volatile organic compounds by devolatilization. *Ind Eng Chem Res*. 2005;44:4042–4050.
6. Ilundain P, Salazar R, Alvarez D, Da Cunha L, Barandiaran MJ, Asua JM. Modeling and optimization of postpolymerization processes. *Ind Eng Chem Res*. 2004;43:1244–1250.
7. Tillier DL, Meuldijk J, Koning CE. Production of colloidally stable latices from low molecular weight ethylene–propylene–diene copolymers. *Polymer* 2003;44:7883–7890.
8. Gamlin CD, Dutta NK, Choudhury NR. Mechanism and kinetics of the isothermal thermodegradation of ethylene-propylene-diene (EPDM) elastomers. *Polym Degrad Stab*. 2003;80:525–531.
9. Allen RD. Fundamentals of compounding Epdm for cost/performance. *J Elastom Plast*. 1983;15:19–32.
10. Li R, Corripio AB, Dooley KM, Henson MA, Kurtz MJ. Dynamic modeling of crosslinking and gelation in continuous ethylene–propylene–diene polymerization reactors using the pseudo–kinetic constant approach. *Chem Eng Sci*. 2004;59:2297–2313.
11. Noordermeer JW. Ethylene–propylene elastomers. In: Othmer K, editor. *Encyclopedia of Polymer Science and Technology*. Hoboken: Wiley-Interscience, 2002:704–719.
12. Ravishankar P. Treatise on EPDM. *Rubber Chem Technol*. 2012;85: 327–349.
13. Ver Strate G. Coordination polymerization. In: Kroswitz J, editor. *Concise Encyclopedia of Polymer Science Engineering*. New York: Wiley-Interscience, 1990:359–362.
14. Quadri G. Purification of polymers from solvents by steam or gas stripping. *Ind Eng Chem Res*. 1998;37:2850–2863.
15. Matthews FJ, Fair JR, Barlow JW, Paul DR, Cozewith C. Solvent removal from ethylene-propylene elastomers. 2. Modeling of continuous-flow stripping vessels. *Ind Eng Chem Prod Res Dev*. 1986;25:65–68.
16. Van Amerongen G. Diffusion in elastomers. *Rubber Chem Technol*. 1964;37:1065–1152.
17. Frensdorff H. Diffusion and sorption of vapors in ethylene–propylene copolymers. II. Diffusion. *J Polym Sci Part A: Polym Chem*. 1964;2:341–355.
18. Cozewith C. Diffusion from spherical particles in a continuous flow stirred tank train. *Ind Eng Chem Res*. 1994;33:2712–2716.
19. Matthews FJ, Fair JR, Barlow JW, Paul DR, Cozewith C. Solvent removal from ethylene-propylene elastomers. 1. Determination of diffusion mechanism. *Ind Eng Chem Prod Res Dev*. 1986;25:58–64.
20. Crank J. *The Mathematics of Diffusion*. Oxford: Oxford University Press, 1979.
21. Francoeur A. A mathematical model for the devolatilization of EPDM rubber in a series of steam stripping vessels. Ph.D. Thesis. Canada: Queen's University, 2012.
22. Levenspiel O. *Chemical Reaction Engineering*. New York: Wiley, 1972.
23. Himmelblau DM, Bischoff KB. Process analysis and simulation: deterministic systems. New York: Wiley, 1968.
24. Thompson DE, McAuley KB, McLellan PJ. Parameter estimation in a simplified MWD model for HDPE produced by a Ziegler-Natta Catalyst. *Macromol React Eng*. 2009;3:160–177.
25. Yao KZ, Shaw BM, Kou B, McAuley KB, Bacon D. Modeling ethylene/butene copolymerization with multi-site catalysts: parameter estimability and experimental design. *Polym React Eng*. 2003;11: 563–588.
26. Wu S, McAuley K, Harris T. Selection of simplified models: I. Analysis of model-selection criteria using mean-squared error. *Can J Chem Eng*. 2011;89:148–158.
27. Wu S, McAuley K, Harris T. Selection of simplified models: II. Development of a model selection criterion based on mean squared error. *Can J Chem Eng*. 2011;89:325–336.
28. McLean KA, McAuley KB. Mathematical modelling of chemical processes—obtaining the best model predictions and parameter estimates using identifiability and estimability procedures. *Can J Chem Eng*. 2012;90:351–366.
29. Barandiaran MJ, Asua JM. Removal of monomers and VOCs from polymers. In: Meyer T, Keurentjes J, editors. Handbook of Polymer Reaction Engineering. Weinheim: Wiley-VCH, 2005:971–994.

Manuscript received Nov. 11, 2013, and revision received Feb. 26, 2014.